

# Crystallization Behavior and Mechanical Properties of Bio-Based Green Composites Based on Poly(L-lactide) and Kenaf Fiber

Pengju Pan,<sup>1</sup> Bo Zhu,<sup>1</sup> Weihua Kai,<sup>1</sup> Shin Serizawa,<sup>2</sup> Masatoshi Iji,<sup>2</sup> Yoshio Inoue<sup>1</sup>

<sup>1</sup>Department of Biomolecular Engineering, Tokyo Institute of Technology, Midori-ku, Yokohama 226-8501, Japan

<sup>2</sup>Fundamental and Environmental Research Laboratories, NEC Corporation, Tsukuba, Ibaraki 305-8501, Japan

Received 11 December 2006; accepted 23 February 2007

DOI 10.1002/app.26407

Published online 23 April 2007 in Wiley InterScience (www.interscience.wiley.com).

**ABSTRACT:** Bio-based polymer composite was successfully fabricated from plant-derived kenaf fiber (KF) and renewable resource-based biodegradable polyester, poly(L-lactide) (PLLA), by melt-mixing technique. The effect of the KF weight contents (0, 10, 20, and 30 wt %) on crystallization behavior, composite morphology, mechanical, and dynamic mechanical properties of PLLA/KF composites were investigated. It was found that the incorporation of KF significantly improves the crystallization rate and tensile and storage modulus. The crystallization of PLLA can be completed during the cooling process from the melt at 5°C/min with the addition of 10 wt % KF. It was also observed that the nucleation density increases dramatically and the spherulite size drops greatly in the isothermal crystallization with the presence of KF. In addition, with the incorporation of 30 wt % KF, the half times of isothermal crystallization at 120°C and 140°C were reduced

to 46.5% and 28.1% of the pure PLLA, respectively. Moreover, the tensile and storage modulus of the composite are improved by 30% and 28%, respectively, by the reinforcement with 30% KF. Scanning electron microscopy observation also showed that the crystallization rate and mechanical properties could be further improved by optimizing the interfacial interaction and compatibility between the KF and PLLA matrix. Overall, it was concluded that the KF could be the potential and promising filler for PLLA to produce biodegradable composite materials, owing to its good ability to improve the mechanical properties as well as to accelerate the crystallization of PLLA. © 2007 Wiley Periodicals, Inc. *J Appl Polym Sci* 105: 1511–1520, 2007

**Key words:** poly(L-lactide); kenaf fiber; biocomposite; crystallization; mechanical properties

## INTRODUCTION

Natural fiber-reinforced plastics, emerging as one kind of benign composite materials, have attracted increasing attention from the standpoint of protection of the natural environments in recent years.<sup>1–3</sup> They have been looked upon as an ecofriendly and economical alternate to glass fibers, owing to the good properties of the natural fibers such as renewability, biodegradability, low cost, low density, acceptable specific mechanical properties, ease of separation, and carbon dioxide sequestration.<sup>3</sup> Natural fiber-reinforced composites have increasing interest in many applications areas including automobile, housing, packaging, and electronic products.<sup>2,4</sup> The composites from natural fibers and conventional polyolefins, that is, polypropylene and polyethylene, have been extensively studied.<sup>5–7</sup> However, the vast use of conventional plastics has induced some envi-

ronmental problems, such as exhausting fossil-based raw materials, nonbiodegradability, and increase in the volume of refuse, etc. Therefore, there is an increasing interest in developing ecofriendly green composites or biocomposites by reinforcing the renewable sources-derived biodegradable plastics with the plant-derived natural fibers.<sup>8–20</sup>

One of the most promising biodegradable polymers is poly(L-lactide) (PLLA), which is producible from renewable resources, such as corn, and non-toxic to human body.<sup>21,22</sup> PLLA has been widely used as a biocompatible polymer for applications in implant materials, surgical suture, and controlled drug delivery systems.<sup>23,24</sup> Moreover, owing to its good mechanical properties and versatile fabrication processes, PLLA also has tremendous potential in traditional applications where common thermoplastics are employed, such as industrial devices, packaging, and film and fiber materials.<sup>25,26</sup> On the other hand, kenaf fiber (KF) has recently been gaining a lot of attention as biomass-based additive, and it is well known as a cellulosic source with ecological and economical advantages, exhibiting low density, nonabrasiveness during processing, high-specific mechanical properties, and biodegradability. It has

Correspondence to: Y. Inoue (inoue.y.af@m.titech.ac.jp).

been reported that KF has a significantly high ability to accumulate carbon dioxide. Its photosynthesis speed is at least three times higher than that of usual plants, and it can absorb carbon dioxide 1.4 times that of its own weight.<sup>27</sup> KF has been mainly used for textiles and paper before, and recently composites of KF and plastics have been studied owing to its promising properties.<sup>4,9,28,29</sup>

PLLA is a relatively stiff and rigid polymer characterized by high mechanical strength and modulus among the family of environmentally friendly biodegradable polymers. However, PLLA is too brittle, for example in the tensile test, the elongation ratio is only about 5%. In addition, the crystallization of PLLA is too slow, which is not convenient for processing. Furthermore, as one of the promising thermoplastics at present, the cost of PLLA is too high. These drawbacks have limited its commercial applications to some extent. Therefore, it is considered that reinforcing PLLA with KFs is possibly an efficient way to enhance its mechanical and thermal properties, as well as to improve its crystallization rate and decrease the cost of PLLA-based materials.

The objective of this work is to fabricate the green composite from KF and PLLA by the melt-mixing technique, and to investigate the effect of fiber weight contents on the nonisothermal and isothermal crystallization behavior, mechanical, and dynamical mechanical thermal properties. Moreover, to study the influence of KF on the crystallization process of PLLA, the isothermal crystallization kinetics and the crystalline morphology of KF-reinforced PLLA composite with different KF contents were also analyzed.

## EXPERIMENTAL

### Materials

Poly(L-lactide) (PLLA; trade name: LACTY 9020; molecular weight:  $M_w = 123,000$ , as reported by the manufacturer) was obtained from Shimadzu (Kyoto, Japan). KF (average length = 3 mm, average diameter = 25  $\mu\text{m}$ , specific gravity = 1.48) was kindly supplied by Fundamental and Environmental Research Laboratory, NEC (Ibaraki, Japan).

### Preparation of composites

PLLA and KF were dried for 2 days at 40°C in a vacuum oven before processing. The composites were fabricated by blending PLLA and KF in single screw machine (Imoto Machinery, Kyoto, Japan) with a speed of 80 rpm at 200°C for 3 min, and then the mixture was injected. The composite was hot-pressed at 200°C after melting for 2 min, and then the hot-pressed sample was quenched to 25°C under

room conditions. The composites are denoted as PLLA/KF ( $x/y$ ), where  $x$  and  $y$  are the weight percentages of PLLA and KF, respectively.

### Measurements

#### Differential scanning calorimeter

The nonisothermal and isothermal crystallization behavior of the pure PLLA and PLLA/KF composites were studied using a Pyries Diamond differential scanning calorimeter (DSC) instrument (Perkin-Elmer Japan, Tokyo, Japan). The scales of temperature and heat flow at different heating rates were calibrated using an indium standard with nitrogen purging. PLLA and composite samples were weighted and sealed in an aluminum pan. In the isothermal melt-crystallization, the melted samples were cooled at a rate of 100°C/min to the desired  $T_c$  after melting at 200°C for 2 min and allowed to crystallize. In the nonisothermal melt-crystallization, the melted samples were cooled to 0°C at various rates after melted in the same conditions. Then, the crystallized sample was heated to 200°C at 10°C/min to observe the melting behavior. In the measurement of the glass transition temperature ( $T_g$ ), the sample was at first quenched to 0°C with a cooling rate of 100°C/min after melting at 200°C for 2 min, and then it was heated at a rate of 10°C/min.

#### Wide-angle X-ray diffraction

The wide-angle X-ray diffraction (WAXD) analysis for the pure PLLA and PLLA/KF composites were carried out on a Rigaku RU-200 (Rigaku, Tokyo, Japan), working at 40 kV and 200 mA, with Ni-filtered Cu K $\alpha$  radiation ( $\lambda = 0.15418$  nm). Scans were made between Bragg angles of 5–50° at a scanning rate of 1°/min.

#### Thermogravimetric analysis

Thermogravimetric analysis (TGA) was performed by Seiko (Tokyo, Japan) TG/DTA 220U with the Exstar 6000 Station. The samples were scanned from 30 to 600°C at a heating rate of 5°C/min in the presence of nitrogen flow.

#### Tensile testing

Tensile properties were measured with the help of Shimadzu EZ test machine at a crosshead speed of 2 mm/min. All the samples have a gauge length of 22.25 mm and a gauge width of 4.76 mm, with variable thickness in the range of 0.35–0.40 mm. Each value of mechanical properties reported was an average of seven specimens. The Young's modulus

**TABLE I**  
Detailed Information Obtained from DSC Thermal Analysis of PLLA and Its Composites

Sample	$T_g$ (°C)	$T_c$ (°C)	$\Delta H_c$ (J/g PLLA)	$T_m$ (°C)	$\Delta H_m$ (J/g PLLA)	$X_c$ (%)
PLLA	58.4	97.7	-16.6	169.6	43.1	53.0
PLLA/KF (90/10)	58.2	101.4	-37.5	170.2	47.2	58.1
PLLA/KF (80/20)	58.3	102.6	-38.5	170.3	46.3	56.9
PLLA/KF (70/30)	58.5	103.2	-36.9	170.6	44.5	54.7

$E$  was obtained from the tangent of the initial slope of the stress versus strain curve.

#### Dynamic mechanical thermal analysis

The storage modulus ( $E'$ ), loss modulus ( $E''$ ), and loss factor ( $\tan \delta$ ) of the pure PLLA and the composites were measured as a function of temperature (-10 to 180°C) using a DMS210 (Seiko) equipped with SSC5300 controller at a frequency of 5 Hz and a heating constant rate of 2°C/min. The samples were thin rectangular strips with dimensions of about 30 × 10 × 0.4 mm<sup>3</sup>.

#### Scanning electron microscopy

A JEOL scanning electron microscope (SEM; model JSM-5200) was used to evaluate the morphologies of fractured surfaces of pure PLLA and the composites. The samples were sputter-coated with gold particles up to a thickness of about 10 nm before the surface characterization.

## RESULTS AND DISCUSSION

### Nonisothermal crystallization behavior

The nonisothermal melt-crystallization with a cooling rate of 5°C/min and the subsequent melt behavior at 10°C/min of neat PLLA and PLLA/KF composites were investigated by DSC. The thermal properties, such as the glass transition temperature ( $T_g$ ), crystallization temperature ( $T_c$ ), melting temperature ( $T_m$ ), crystallization enthalpy ( $\Delta H_c$ ), and melting enthalpy ( $\Delta H_m$ ) obtained from DSC analysis, are summarized in Table I. The degree of crystallinity ( $X_c$ %) of neat PLLA and PLLA in the composites was obtained by comparing the melting enthalpy ( $\Delta H_m$ ) with the value of an infinitely large crystal ( $\Delta H_m^0$ ), taken as  $\Delta H_m^0 = 81.3 \text{ J/g}^{30}$  ( $X_c = \Delta H_m / \Delta H_m^0 \times 100\%$ ). Table I indicates that the  $T_g$  values of the composites do not change obviously with the addition of KF to the PLLA matrix. In Figure 1, the neat PLLA sample shows a smaller crystallization peak ( $\Delta H_c = -16.6 \text{ J/g}$ ) during the cooling process, and it shows a cold crystallization peak appearing at around 105°C in the subsequent heating, indicating that the crystallization of PLLA does not complete in the cooling process at 5°C/min. However, no cold crystallization

peak is observed in the DSC heating curves of the composites, demonstrating that PLLA almost crystallizes fully in the composites during the cooling process. Moreover, the crystallization peak of PLLA shifts to higher temperature with the incorporation of KF, signifying that the crystallization rate of PLLA is enhanced with the presence of KF.

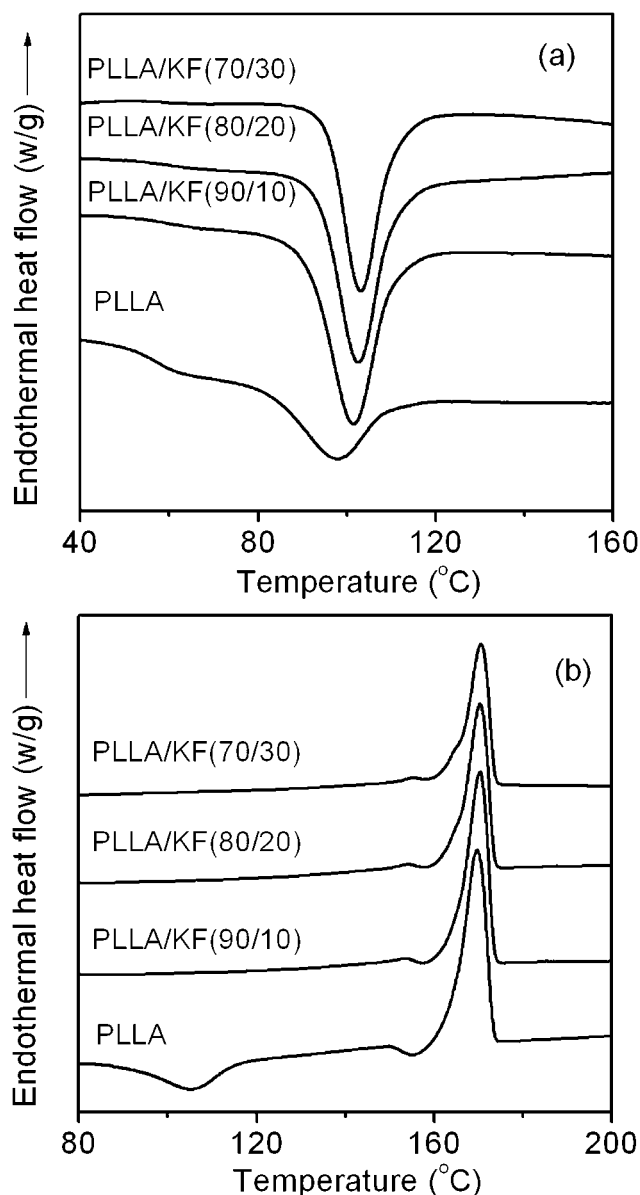


**Figure 1** DSC curves of (a) nonisothermal melt-crystallization with a cooling rate of 5°C/min and (b) subsequent heating scanning at 10°C/min of PLLA and its composites.

In general, the crystallization process of polymers from the melted state can be divided into two stages, that is, the nucleation and the crystal growth. A primary nucleation process may be either homogeneous or heterogeneous.<sup>31</sup> The homogeneous nucleation occurs sporadically in the melt by thermal fluctuation, whereas the heterogeneous one starts on the surface of microscopic insoluble particles dispersed randomly in the polymer melt, such as impurities or nucleating agents arbitrarily added. In practice however, unless under very special conditions, it is rare to observe homogeneous nucleation for crystalline polymers. Whenever there is nucleating agent present in a polymer melt, it can affect the free energy balance for nucleation, usually, so as to increase the nucleation rate and prevent homogeneous nucleation. For heterogeneous nucleation, owing to a much reduced surface energy, the nucleation rate can increase by several orders of magnitude. Therefore, the effect of homogeneous nucleation can be totally smeared by heterogeneous nucleation.<sup>32,33</sup>

As for polymeric composite system, there are two main factors controlling the crystallization process.<sup>13,34</sup> First, the additives, which have a nucleating effect on the crystallization, enhance the crystallization, and so they have a positive influence on the degree of crystallinity. Second, the additives, which have a negative effect on the crystallization, hinder the migration and diffusion of polymeric molecular chains to the surface of the growing face of the polymer crystal in the composites, resulting in a decrease in the crystallization rate. Owing to the nucleation effect of KF, the crystallization rate was improved dramatically in the presence of KF. Nevertheless, because of the hindrance of polymer diffusion by KF, for the PLLA/KF composites, the  $T_c$  value only increases a little with the increase of KF content. Besides, Table I also shows that when the KF content is larger than 10 wt %, as KF content increases the degree of crystallinity of the composites reduces, signifying that the KF fibers hinder the migration and diffusion of PLLA molecular chains to the surface of the nucleus in the composites. Similar results were also observed in the case of PLLA/talc (70/30) composite.<sup>12</sup> Usually, at higher  $T_c$ , the developed lamellar has a higher melting temperature in the crystallization of polymer. Therefore, as KF content increases because of the increase of the  $T_c$  value, the  $T_m$  value also increases at the same time.

### Isothermal crystallization behavior

The isothermal crystallization behavior of neat PLLA and PLLA/KF composites at 120°C and 140°C was also surveyed by DSC, and the results are presented in Figure 2(a,b), respectively. Clearly, the isothermal crystallization of composites is much faster than that

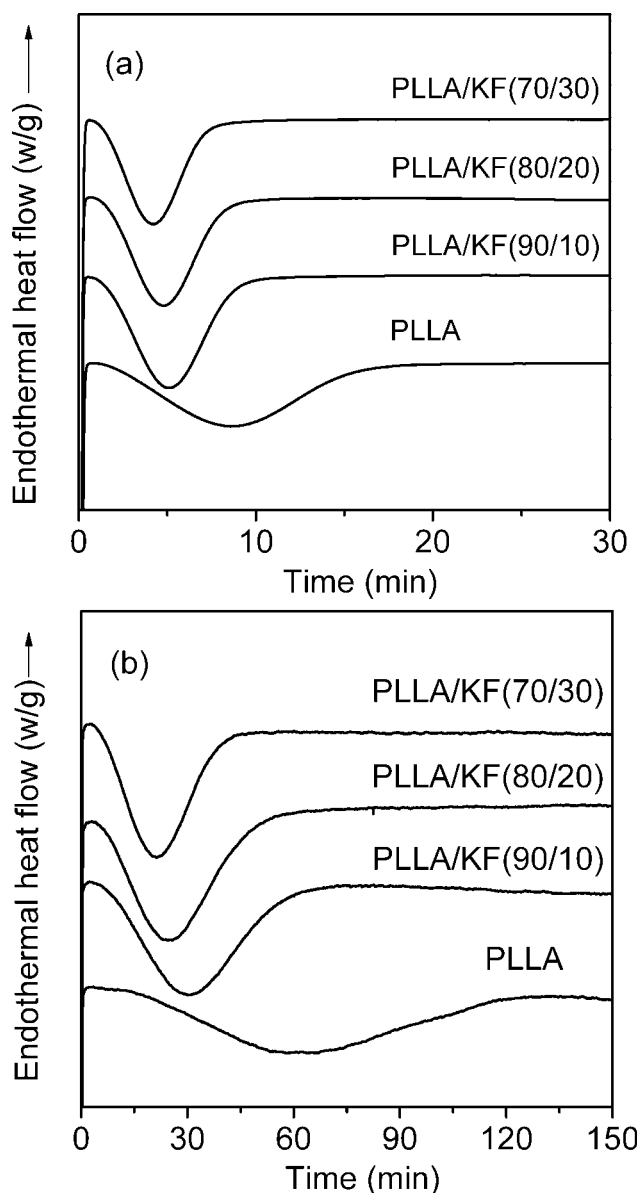


**Figure 2** Isothermal melt-crystallization DSC curves of PLLA and its composites at (a) 120°C and (b) 140°C.

of the pure PLLA, confirming that the crystallization rate of PLLA is effectively enhanced with the addition of KF. Moreover, the crystallization kinetics was analyzed from the isothermal DSC measurements. The isothermal heat flow curve was integrated to determine the degree of crystallinity of the samples as a function of crystallization time. The relative crystallinity ( $X_t$ ) at any given time was calculated from the integrated area of the DSC curve from  $t = 0$  to  $t = t$  divided by the integrated area of the whole heat flow curve.

The isothermal bulk crystallization kinetics was analyzed with the Avrami equation<sup>35,36</sup>:

$$X_t = 1 - \exp(-kt^n) \quad (1)$$

**TABLE II**  
Kinetic Parameters of Isothermal Crystallization at 120°C and 140°C of Neat PLLA and Its Composites

Sample	$T_c = 120^\circ\text{C}$				$T_c = 140^\circ\text{C}$			
	$t_{1/2}$ (min)	$\Delta H_c$ (J/g PLLA)	$n$	$\log k$	$t_{1/2}$ (min)	$\Delta H_c$ (J/g PLLA)	$n$	$\log k$
PLLA	7.95	-45.5	2.64	-2.53	60.23	-56.0	2.87	-5.27
PLLA/KF (90/10)	4.73	-49.1	2.89	-2.11	29.05	-60.5	2.66	-4.05
PLLA/KF (80/20)	4.22	-47.5	2.95	-2.01	23.23	-59.4	2.48	-3.55
PLLA/KF (70/30)	3.70	-46.0	2.94	-1.83	16.93	-55.8	2.43	-3.14

where  $n$  is an index related to the dimensional growth and the way of formation of primary nuclei, and  $k$  is the overall rate constant associated with both nucleation and growth contributions. The linear form of Eq. (1) is given as Eq. (2):

$$\log[-\ln(1 - X_t)] = \log k + n \log t \quad (2)$$

The values of  $n$  and  $k$  are obtained by plotting  $\log[-\ln(1 - X_t)]$  against  $\log t$ . Meanwhile, the crystallization half-time  $t_{1/2}$ , which is defined as the time when the crystallinity arrives at 50%, can be determined from the kinetics parameters measured by using the following equation:

$$t_{1/2} = \left(\frac{\ln 2}{k}\right)^{1/n} \quad (3)$$

The crystallization parameters  $k$ ,  $n$ , and  $t_{1/2}$  of neat PLLA and PLLA/KF composites crystallized at 120°C and 140°C are listed in Table II. Owing to the heterogeneous nucleation effect of KF on the crystallization of PLLA, the  $t_{1/2}$  reduces significantly in the presence of KF, and the  $t_{1/2}$  of PLLA/KF (70/30) composite crystallized at 120°C and 140°C reduces to 46.5% and 28.1% of the pure PLLA, respectively. The Avrami exponent  $n$  is similar for the pure PLLA and its composites at a given isothermal crystallization temperature. However, the Avrami rate constant  $k$  increases with the increasing KF content. Corresponding quite well with the nonisothermal DSC results, because of the hindrance of polymer diffusion by KF, the crystallization enthalpy of the PLLA/KF composites decreases as the KF content increases when the KF contents are larger than 10 wt %. Owing to the more ordered crystal developed at higher  $T_c$

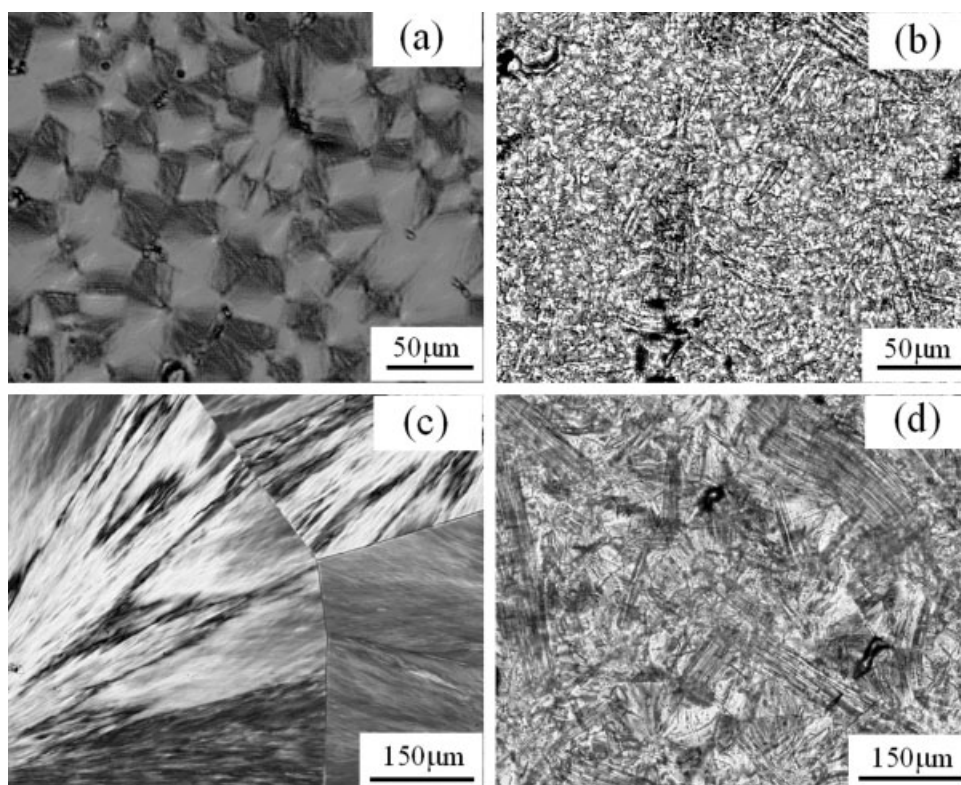


**Figure 3** Optical micrographs of neat PLLA (a,c) and PLLA/KF (80/20) composite (b,d) isothermally melt-crystallized at 120°C (a, b) and 140°C (c,d).

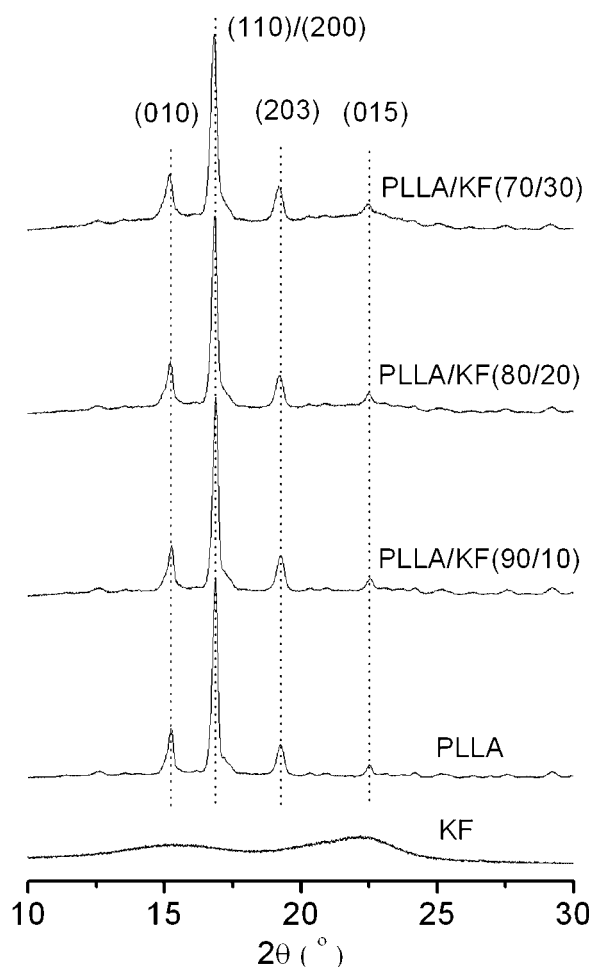


**Figure 4** WAXD patterns of kenaf fiber, neat PLLA, and PLLA/KF composites isothermally melt-crystallized at 140°C.

the crystallization enthalpy of PLLA and its composites crystallized at 140°C is larger than that of those crystallized at 120°C.

The spherulite morphology of pure PLLA and PLLA/KF (80/20) composite isothermally melt-crystallized at 120°C and 140°C were also observed by polarizing optical microscopy (POM), respectively, and the results are shown in Figure 3. It is obvious that with the addition of KF the nucleation density increases greatly and the spherulite size drops drastically at both 120°C and 140°C, which confirms that the KF can significantly accelerate the nucleation and crystallization of PLLA. On the other hand, the nucleation density reduces and the spherulite size increases, with the increase of the crystallization temperature.

The crystalline structure of the neat PLLA and PLLA/KF composites after isothermal crystallization at 140°C, as well as the structure of KF used in this study were investigated using WAXD, as shown in Figure 4. KF shows two weak diffraction peaks at around  $2\theta = 15.4^\circ$  and  $22.2^\circ$ , indicating that KF is

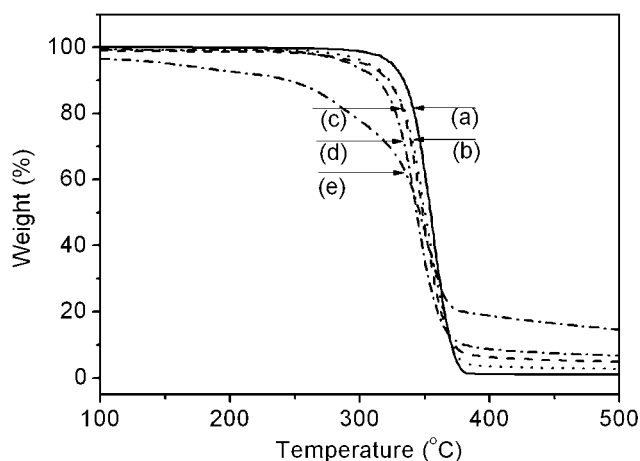


**Figure 5** TGA curves of neat PLLA, KF, and PLLA-KF composites: (a) neat PLLA, (b) PLLA/KF (90/10), (c) PLLA/KF (80/20), (d) PLLA/KF (70/30), and (e) KF.

belonging to cellulous I type fiber, though the crystallinity seems to be relatively low.<sup>9</sup> The neat PLLA and its composites all exhibit very strong reflections at around  $2\theta = 15.3^\circ$ ,  $16.8^\circ$ , and  $19.3^\circ$  due to the diffraction from (010), (110)/(200), and (203) planes, respectively.<sup>37</sup> No obvious differences related to the diffraction peaks and peak positions were observed between the neat PLLA and its composites, signifying that the crystalline structure of PLLA crystallized at 140°C is almost not affected by the addition of KF.

### Thermogravimetric analysis

The thermal stability of pure PLLA, KF, and their composites was investigated with TGA, and the results are shown in Figure 5. In Table III, the 5%, 25%, 50%, 75% weight-loss temperatures ( $T_5$ ,  $T_{25}$ ,  $T_{50}$ , and  $T_{75}$ , respectively) are also listed for all specimens shown in Figure 5. Similar with the decomposition behavior of other plant fibers, such as the bamboo fiber and the recycled newspaper fiber,<sup>13,14</sup> KF degrades in three stages. The first stage (40–140°C) is due to the release of absorbed moisture in the fibers, even after the 48 h of drying was conducted to eliminate moisture. The second transition (140–370°C) is related to the degradation of cellulosic substances such as hemicelluloses and cellulose. In

**TABLE III**  
TGA Characterization of Neat PLLA, KF, and PLLA/KF Composites

Sample	$T_5$ (°C)	$T_{25}$ (°C)	$T_{50}$ (°C)	$T_{75}$ (°C)
PLLA	323	345	354	363
KF	154	309	346	364
PLLA/KF (90/10)	307	339	350	361
PLLA/KF (80/20)	303	337	348	359
PLLA/KF (70/30)	293	332	344	356

**TABLE IV**  
Tensile Properties of Neat PLLA and PLLA/KF Composites

Sample	Tensile strength (MPa)	Tensile modulus (GPa)	Fracture strain (%)
PLLA	47.4 ± 2.5	1.43 ± 0.06	6.25 ± 0.52
PLLA/KF (90/10)	39.2 ± 1.7	1.60 ± 0.08	2.82 ± 0.19
PLLA/KF (80/20)	37.1 ± 1.9	1.73 ± 0.11	2.26 ± 0.21
PLLA/KF (70/30)	35.5 ± 2.1	1.86 ± 0.10	1.95 ± 0.12

this stage, only small amount of KF is degraded below 250°C, and the degradation rate of KF is more drastic after 250°C. The third stage (370–600°C) of the decomposition is due to the degradation of non-cellulosic materials in the fiber, and in this stage the relationship between weight and temperature is almost linear. The thermal stability of pure PLLA is better than that of KF, and the onset temperature of thermal degradation of PLLA is about 310°C. Therefore, the thermal stability of the PLLA/KF composites decreases when compared with the pure PLLA, and as the KF content increases, the onset temperature of thermal degradation of the composites also reduces.

### Tensile properties

The tensile strength, modulus, and fracture strain of neat PLLA and PLLA/KF composites are listed in Table IV. Comparison between the tensile stress–strain curves of pure PLLA and its composites with different KF contents is shown in Figure 6. The pure PLLA film has a tensile strength of 47.4 MPa, a

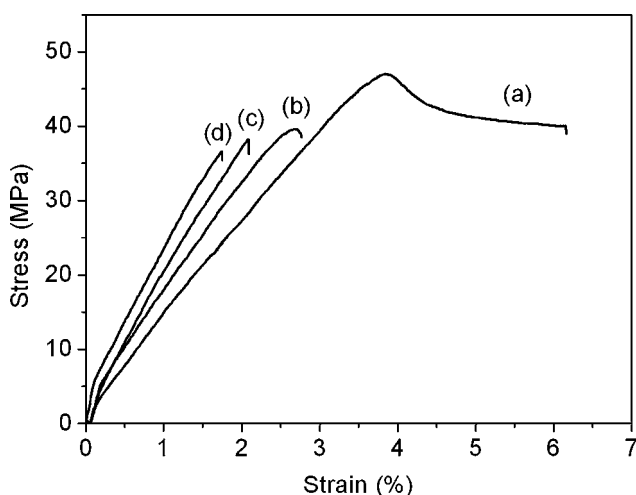


**Figure 6** Stress–strain curves of neat PLLA and PLLA/KF composites: (a) neat PLLA, (b) PLLA/KF (90/10), (c) PLLA/KF (80/20), and (d) PLLA/KF (70/30).

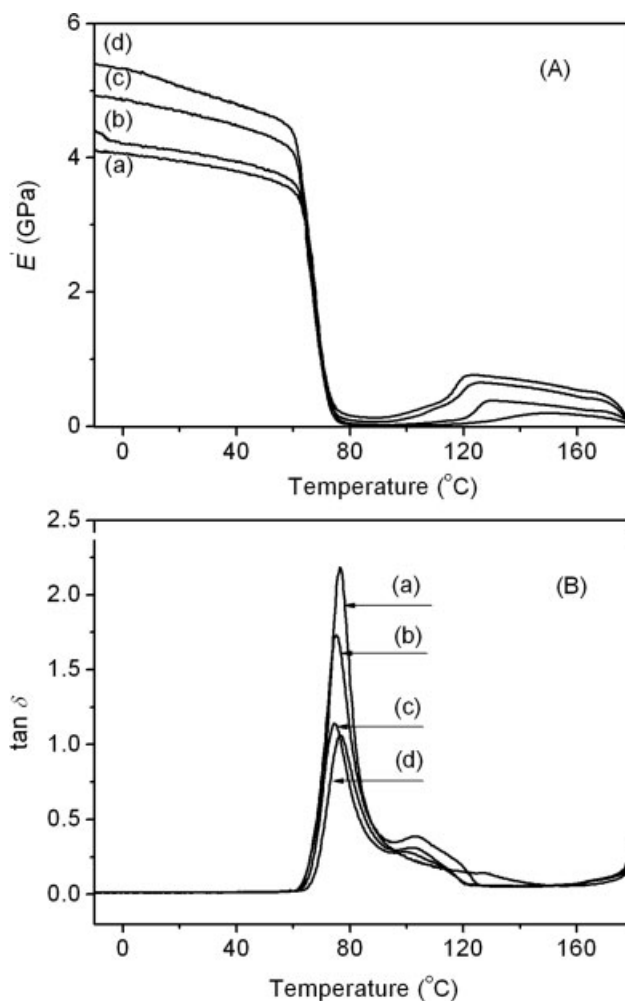


**Figure 7** Temperature dependence of (A) storage modulus and (B)  $\tan \delta$  of neat PLLA and PLLA/KF composites: (a) neat PLLA, (b) PLLA/KF (90/10), (c) PLLA/KF (80/20), and (d) PLLA/KF (70/30).

modulus of 1.43 GPa, and a fracture strain of 6.25%. During tensile testing, the specimen fractured suddenly after the yield point and the neck was not observed, indicating the brittleness of PLLA. As presented in Table IV, the addition of KF improves the modulus of PLLA, signifying that stress transfers from the PLLA matrix to the stiffer fiber occurred.<sup>38</sup> The tensile modulus of the PLLA/KF composites containing 20 and 30 wt % KF increases by 21% and 30%, respectively, when compared with the pure PLLA.

Though the addition of KF increases the modulus, the tensile strength as well as the fracture strain of the composites shows a decrease with the increase of KF content. This could be the result of less adequate adhesion between KF and PLLA, leading to the poor interface interaction. Generally, the addition of high fiber content increases the probability of fiber agglomeration, which creates regions of stress concentrations that require less energy to elongate the crack

**TABLE V**  
Storage Modulus of Neat PLLA and PLLA/KF Composites

Sample	$E'$ at 0°C (GPa)	$E'$ at 25°C (GPa)	$E'$ at 40°C (GPa)	$E'$ at 58°C (GPa)
PLLA	4.06	3.92	3.79	3.57
PLLA/KF (90/10)	4.26	4.07	3.94	3.66
PLLA/KF (80/20)	4.87	4.65	4.47	4.17
PLLA/KF (70/30)	5.33	5.01	4.81	4.49

propagation.<sup>12</sup> During tensile deformation, the stress cannot transfer efficiently nearby these flaws, resulting in the failure of the specimen before the yield. On the other hand, in the composite, all the elongation arises from the polymer, since KF is rigid relative to PLLA. Hence, increasing the amount of filler decreases the amount of polymer available for elongation and reduces the failure strain. These tensile results show that the brittleness of PLLA containing KF is not significantly improved due to the less adequate adhesion between the fiber and the polymer. So it is considered that modification of fiber by using compatibilizers or coupling agents is possible to improve the toughness of composites.

#### Dynamic mechanical thermal analysis

The temperature dependence of the storage modulus ( $E'$ ) and  $\tan \delta$  of pure PLLA and PLLA/KF composites is shown in Figure 7(A,B), respectively. Storage modulus represents the ratio of the in-phase stress to the applied strain, which is further related to the energy stored per cycle of deformation. Storage modulus determines the dynamic rigidity of a material, which originates from the elastic response of the material. The values of  $E'$  of PLLA and the composites at 0°C, 25°C, 40°C, and 58°C (nearby  $T_g$ ) were summarized in Table V. It is distinct from Figure 7(A) and Table V that  $E'$  of the material increases in the presence of KF, and also as KF content increases  $E'$  of the composites improves. The  $E'$  values of the

PLLA/KF composites containing 20 and 30 wt % KF increase by 19% and 28%, respectively, when compared with those of neat PLLA at 25°C. Besides, the  $E'$  values decrease for both the pure PLLA and the composites with increasing temperature due to the softening of the PLLA matrix. On the other hand, with the addition of the KF fiber, the improvement of the storage modulus as well as the tensile modulus is smaller than the results published for the cellulose fibers-reinforced biodegradable composites.<sup>8,12</sup> This is probably because the shapes of the tested specimens are different with those in the references,<sup>8,12</sup> and in this study, the specimens for both tensile testing and dynamic mechanical thermal analysis (DMTA) are in the film state in which the fibers are oriented to the film plane during hot-pressing.

As shown in Figure 7(B), the height of the  $\tan \delta$  peak decreases with the presence of KF. One possible explanation of this phenomenon is that the neat PLLA shows a sharp and intense peak because there is no restriction to the chain motion, while the presence of KF hinders the chain mobility, leading to the reduction of sharpness and height of the  $\tan \delta$  peak.<sup>12,39</sup> Furthermore, the damping in the transition region measures the imperfections in the elasticity, and much of the energy used to deform a material during DMTA testing is dissipated directly as heat.<sup>40</sup> Hence, the molecular mobility of the composites decreases, and the mechanical loss to overcome intermolecular chain friction is reduced with the addition of the KFs. It is also considered that the reduction in  $\tan \delta$  also denotes an improvement in the hysteresis of the system and a reduction in the internal friction.<sup>41</sup>

#### Morphology of composites

The morphologies of KF and PLLA/KF composites were evaluated by means of SEM. The SEM micrographs of the KF are shown in Figure 8. The SEM micrographs reveal large-scale variations in the aspect ratio, diameter, and the morphology of KF. It

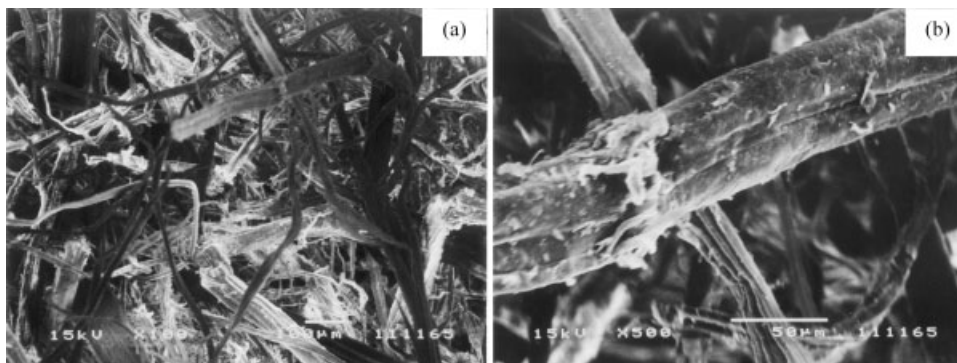


**Figure 8** SEM micrographs of the kenaf fiber: (a)  $\times 100$  and (b)  $\times 500$ .



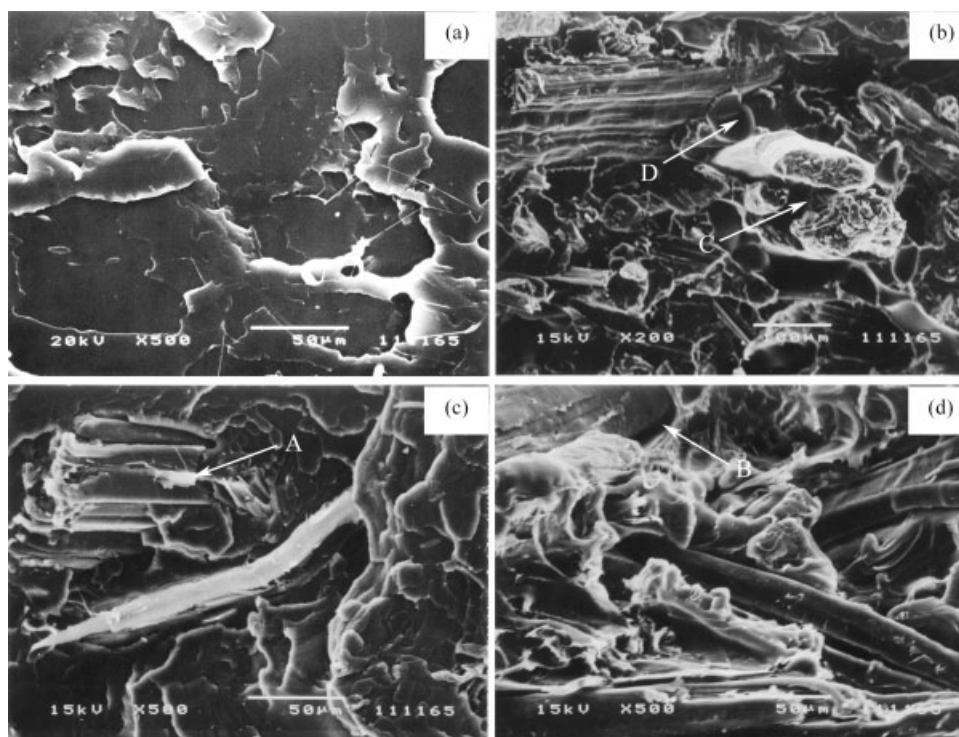


**Figure 9** SEM micrographs of the fracture surface of (a) pure PLLA and the PLLA/KF (70/30) composites: (b)  $\times 200$ , (c)  $\times 500$  and (d)  $\times 500$ .

is observed that the diameters of the fibers ranges from 5 to 50  $\mu\text{m}$ , and the surface of the fibers is rough with the adhesion of some smaller fibers and particles. These variations are probably accounted to the different sources and the processing history of the fibers presented in the composition of KF.

SEM micrographs of the tensile-fractured surfaces of the pure PLLA and PLLA/KF (70/30) composite are presented in Figure 9. The fracture surface of pure PLLA is irregular and rough, besides no craze and fibril is observed in the surface, revealing that the fracture of PLLA is in a "brittle" manner.<sup>42</sup> Similar with the pure PLLA, the fracture surface of composite also illustrates its brittleness. Owing to the variability in the morphology of the KF, the SEM micrographs are not able to provide much information regarding the fiber dispersion and the interface interaction between fibers and polymer matrix.

It is observed that in the composites the most fibers (indicated by "A") are tight connected with the matrix, and a lot of fibers are broken during tensile testing. It is probable that the fiber surface has been covered with a thin layer of the matrix, as fibrils linking the fiber surface to the matrix can be seen in Figure 9(c), which may lead to better stress transfer between the matrix and the reinforcing fibers. However, there are also some fibers (indicated by "B") separating from the matrix during tensile deformation, signifying that the interface interaction between the fibers and polymer matrix can be

further improved. It has been reported that the melting viscosity of PLLA is higher.<sup>43</sup> In addition, as observed by SEM, the surface of KF is rough and irregular. Therefore, because of the high viscosity of the composite system with the incorporation of 30 wt % KF, the aggregation of KFs (indicated by "C") and the presence of small amount of air bubbles (indicated by "D") are also observed in the composites. The mechanical properties of composite greatly depend on the state of the filler dispersion and the strength of the interfacial interaction. It has also been reported that the interfacial interaction between bulk polymer and nucleating agent affects the crystallization rate greatly.<sup>44</sup> Hence, it is considered that the mechanical properties as well as the crystallization behavior can be further optimized through the use of compatibilizers or coupling agents to improve the interface interaction and the compatibility between the KF and PLLA matrix.

## CONCLUSION

In this study, the low-cost, value-added biodegradable composite from PLLA and KF was fabricated, and its properties, particularly crystallization behavior and mechanical properties, were investigated. The incorporation of KF brings considerable improvement in the properties of PLLA such as crystallization rate and tensile and storage modulus. SEM

observation reveals that most KF are well connected with the matrix, but it also shows that the fiber dispersion and interfacial interaction between the fiber and polymer can be further improved. Therefore, it is considered to be able to further enhance the crystallization rate and mechanical properties of PLLA/KF composites by optimizing the interface interaction and compatibility between the KF and PLLA matrix. Hence, the use of KF, as reinforcements in PLLA to produce biodegradable composites, can provide a sustainable alternative to conventional thermoplastic-based materials. Future work will concentrate on efforts to optimize the crystallization process and mechanical properties, and to evaluate the biodegradability of this developing and promising composite.

## References

- Bledzki, A. K.; Gassan, J. *Prog Polym Sci* 1999, 24, 221.
- Saheb, D. N.; Jog, J. P. *Adv Polym Technol* 1999, 18, 351.
- Mohanty, A. K.; Misra, M.; Drzal, L. T. *J Polym Environ* 2002, 10, 19.
- Serizawa, S.; Inoue, K.; Iji, M. *J Appl Polym Sci* 2006, 100, 618.
- Sain, M. M.; Kokta, B. V. *J Appl Polym Sci* 1994, 54, 1545.
- Sanadi, A. R.; Caufield, D. F.; Jacobson, R. E.; Rowell, R. M. *Ind Eng Chem Res* 1995, 34, 1889.
- Lu, J. Z.; Wu, Q.; Negulescu, I. I. *J Appl Polym Sci* 2005, 96, 93.
- Bhardwaj, R.; Mohanty, A. K.; Drzal, L. T.; Pourboghrat, F.; Misra, M. *Biomacromolecules* 2006, 7, 2044.
- Nishino, T.; Hirao, K.; Kotera, M.; Nakamae, K.; Inagaki, H. *Compos Sci Technol* 2003, 63, 1281.
- Wong, S.; Shanks, R. A.; Hodzic, A. *Macromol Mater Eng* 2004, 289, 447.
- Shibata, M.; Ozawa, K.; Teramoto, N.; Yosomiya, R.; Takeishi, H. *Macromol Mater Eng* 2003, 288, 35.
- Huda, M. S.; Mohanty, A. K.; Drzal, L. T.; Schut, E.; Misra, M. *J Mater Sci* 2005, 40, 4221.
- Huda, M. S.; Drzal, L. T.; Misra, M.; Mohanty, A. K.; Williams, K.; Mielewski, D. F. *Ind Eng Chem Res* 2005, 44, 5593.
- Kori, Y.; Kitagawa, K.; Hamada, H. *J Appl Polym Sci* 2005, 98, 603.
- Shin, Y. F.; Lee, W. C.; Jeng, R. J.; Huang, C. M. *J Appl Polym Sci* 2006, 99, 188.
- Shibata, M.; Oyamada, S.; Kobayashi, S.; Yaginuma, D. *J Appl Polym Sci* 2004, 92, 3857.
- Iannace, S.; Nocilla, G.; Nicolais, L. *J Appl Polym Sci* 1999, 73, 583.
- Shibata, M.; Takachiyo, K.; Ozawa, K.; Yosomiya, R.; Takeishi, H. *J Appl Polym Sci* 2002, 85, 129.
- Keller, A. *Compos Sci Technol* 2003, 63, 1307.
- Wong, S.; Shanks, R.; Hodzic, A. *Compos Sci Technol* 2004, 64, 1321.
- Tsuji, H. In *Biopolymers*, Vol. 4: Polyesters III; Doi, Y.; Steinbüchel, A., Eds.; Wiley-VCH: Weinheim, 2002, p 129.
- Drumright, R. E.; Gruber, P. R.; Henton, D. E. *Adv Mater* 2000, 12, 1841.
- Ikada, Y.; Tsuji, H. *Macromol Rapid Commun* 2000, 21, 117.
- Jain, R. A. *Biomaterials* 2000, 21, 2475.
- Sinclair, R. G. *Pure Appl Chem* 1996, A33, 585.
- Aou, K.; Hsu, S. L. *Macromolecules* 2006, 39, 3337.
- Lam, T.; Hori, K.; Iiyama, K. *J Wood Sci* 2003, 49, 255.
- Wambua, P.; Ivens, J.; Verpoest, I. *Compos Sci Technol* 2003, 63, 1259.
- Rouison, D.; Sain, M.; Couturier, M. *Compos Sci Technol* 2004, 64, 629.
- Kalb, B.; Penings, A. *J Polymer* 1980, 21, 607.
- He, Y.; Zhu, B.; Kai, W.; Inoue, Y. *Macromolecules* 2004, 37, 3337.
- Hoffman, J. D.; Davis, G. T.; Lauritzen, J. L. In *Treatise on Solid State Chemistry*; Hannay, N. B., Ed.; Plenum: New York, 1976, p 497.
- Hoffman, J. D. *Polymer* 1983, 24, 3.
- Albano, C.; Papa, J.; Ichazo, M.; Gonzalez, J.; Ustariz, C. *Compos Struct* 2003, 62, 291.
- Avrami, M. *J Chem Phys* 1939, 7, 1103.
- Avrami, M. *J Chem Phys* 1941, 9, 177.
- Miyata, T.; Masuko, T. *Polymer* 1997, 38, 4003.
- Rana, A. K.; Mitra, B. C.; Benerjee, A. N. *J Appl Polym Sci* 1999, 71, 531.
- Pothan, L. A.; Oommen, Z.; Thomas, S. *Compos Sci Technol* 2003, 63, 283.
- Bleach, N. C.; Nazhat, S. N.; Tanner, K. E.; Kellomaki, M.; Tormala, P. *Biomaterials* 2002, 23, 1579.
- Fay, J. J.; Murphy, C. J.; Thomas, D. A.; Sperling, L. H. *Polym Eng Sci* 1991, 31, 1731.
- Lapique, F.; Meakin, P.; Feder, J.; Jossang, T. *J Appl Polym Sci* 2000, 77, 2370.
- Kim, S. H.; Han, Y. K.; Ahn, K. D.; Kim, Y. H.; Chang, T. *Makromol Chem* 1993, 194, 3229.
- Dong, T.; He, Y.; Zhu, B.; Shin, K. M.; Inoue, Y. *Macromolecules* 2005, 38, 7736.